LYMPHOID NEOPLASIA

Activation of hedgehog signaling associates with early disease progression in chronic lymphocytic leukemia

Emanuela M. Ghia,[1] Laura Z. Rassenti,[1] Donna S. Neuberg,[2] Alejandro Blanco,[3] Fouad Yousif,[4] Erin N. Smith,[5] John D. McPherson,[6] Thomas J. Hudson,[4] the HALT Pan-Leukemia Gene Panel Consortium, Olivier Harismendy,[1,7] Kelly A. Frazer,[1,5] and Thomas J. Kipps[1]

[1]Moores Cancer Center, University of California San Diego, La Jolla, CA; [2]Biostatistics and Computational Biology, Dana-Farber Cancer Institute, Boston, MA; [3]Programa de Genetica Humana, Universidad de Chile, Santiago, Chile; [4]Ontario Institute for Cancer Research, Toronto, ON, Canada; [5]Department of Pediatrics and Rady Children's Hospital, University of California San Diego, La Jolla, CA; [6]Department of Biochemistry and Molecular Medicine, UC Davis School of Medicine, Sacramento, CA; and [7]Bioinformatics and Systems Biology, University of California San Diego, La Jolla, CA

KEY POINTS

- A large proportion of patients have CLL cells with activation of Hh signaling leading to expression of GLI1.

- Activation of Hh signaling predicts for relatively short treatment-free survival and sensitivity to GLI1 inhibition.

Targeted sequencing of 103 leukemia-associated genes in leukemia cells from 841 treatment-naive patients with chronic lymphocytic leukemia (CLL) identified 89 (11%) patients as having CLL cells with mutations in genes encoding proteins that putatively are involved in hedgehog (Hh) signaling. Consistent with this finding, there was a significant association between the presence of these mutations and the expression of GLI1 (χ^2 test, $P < .0001$), reflecting activation of the Hh pathway. However, we discovered that 38% of cases without identified mutations also were GLI1$^+$. Patients with GLI1$^+$ CLL cells had a shorter median treatment-free survival than patients with CLL cells lacking expression of GLI1 independent of IGHV mutation status. We found that GANT61, a small molecule that can inhibit GLI1, was highly cytotoxic for GLI1$^+$ CLL cells relative to that of CLL cells without GLI1. Collectively, this study shows that a large proportion of patients have CLL cells with activated Hh signaling, which is associated with early disease progression and enhanced sensitivity to inhibition of GLI1. (*Blood*. 2019;133(25):2651-2663)

Introduction

Whole-exome sequencing of chronic lymphocytic leukemia (CLL) cells has advanced our understanding of this disease.[1-6] Pathway enrichment analyses revealed that the genes found mutated in CLL encoded proteins involved in Notch signaling, inflammation, B-cell receptor signaling, Wnt signaling, chromatin modification, response to DNA damage, cell cycle control, or RNA processing.[1,2,6,7] Finding frequent mutations in clusters of genes involved in these 7 signaling/metabolic pathways implies that they contribute to CLL pathogenesis.[7]

We examined for mutations in 103 genes of the HALT Pan-Leukemia Gene Panel in leukemia cells of 841 treatment-naive patients with CLL. The HALT Pan-Leukemia Gene Panel included genes found mutated in myeloid or lymphoid leukemias and leukemia stem cells.[8] Some genes included in this panel are known to harbor mutations in myeloid leukemia but not in CLL. Reactome pathway enrichment analysis[9] was performed on the genes found to have mutations, with attention focused on those that did not map to these 7 identified signaling/metabolic pathways in CLL.[1,2,6,7]

We detected mutations in genes encoding proteins involved in activation of the Hh signaling pathway. The Hh signaling pathway is a highly conserved regulator of development, tissue patterning, cell proliferation, and differentiation. In mammals, it is activated by the binding of 3 ligands, Sonic Hh (SHh), Desert Hh (DHh), or Indian Hh (IHh), to the transmembrane receptors Patched1 or Patched2 (PTCH1-2).

Loss-of-function mutations in negative regulators, such as *PTCH1-2* or *SUFU*, or gain-of-function mutations in positive regulators, such as *SMO*, can lead to Hh-pathway activation independent of ligand.[10-14] As with ligand-dependent activation,[15] such ligand-independent activation of the Hh pathway leads to overexpression of the main effector of Hh signaling, namely *GLI1*, which serves as a surrogate marker for Hh-pathway activation.[16,17] Consistent with the notion that Hh-pathway activation factors in pathogenesis, overexpression of *GLI1* is an adverse prognostic indicator for patients with acute myeloid leukemia[18] or carcinomas of the breast,[19] ovary,[20] or lung.[21] Moreover, overexpression of *GLI1* is observed in numerous cancer types, including cervical and breast cancers, chronic myeloid leukemia, multiple myeloma, and medulloblastoma.[22-26] Although previous studies noted that CLL cells of some patients have activation of the Hh pathway,[27-30] somatic mutations identified in studies on the genetics of CLL have not been implicated to affect activation of this pathway. We assessed for expression of GLI1 in cases found to harbor mutations in genes that could influence Hh signaling and examined whether activation of this pathway was associated with early disease progression.

Materials and methods

Patient samples

This study was conducted in accordance with the Declaration of Helsinki for the protection of human subjects and the Institutional Review Board of the University of California San Diego (Institutional Review Board approval #110658). Blood samples were collected from 841 patients with CLL enrolled in the CLL Research Consortium upon receipt of written informed consent and who satisfied diagnostic and immunophenotypic criteria for CLL.[31]

Leukemia-associated genes for targeted sequencing

We performed targeted sequencing of the HALT Pan-Leukemia Gene Panel of 103 genes[8] on 841 untreated CLL samples. Briefly, baits were designed to capture the coding sequence of 103 leukemia-associated genes. Illumina sequencing libraries were constructed, and target enrichment was performed by using an Agilent SureSelect kit (Agilent Technologies). The resulting amplified library was quantified and sequenced on the Illumina HiSeq 2000/2500 platform. Reads were aligned to the reference human genome build hg19 using NovoAlign (Novocraft Inc.), and on-target single nucleotide variants and indels were called by using the genome analysis tool kit (GATK). Sequencing data are available through dbGaP (phs000767).

Detection of CLL signaling pathways

Cytoscape software[32] with the Reactome functional interaction (FI) plug-in were used to perform pathway and network-based data analyses[33] with the Reactome FI network,[34] which merges interactions extracted from human-curated pathways with interactions predicted by using a machine learning approach. This approach allowed us to construct an FI network based on sets of genes involved in each of the 7 identified CLL signaling/metabolic pathways.[1,2] Pathway-based data analysis was performed by using Reactome FI and high-quality human-curated pathways in the Reactome database.[35] We also performed Reactome pathway enrichment analysis of the genes found mutated in our study that did not map onto these 7 signaling/metabolic pathways. Pathways with a false discovery rate < 0.05 were considered significantly enriched.

Functional prediction of *Hh-pathway* mutations

PolyPhen-2 software[36] is an automatic tool for prediction of the possible impact of an amino acid substitution on protein function. This prediction is based on a number of features comprising the sequence, phylogenetic, and structural features of the substitution. PolyPhen-2 predicts the functional significance of an amino acid substitution from its individual features by Naive Bayes classifier trained using supervised machine learning. PolyPhen-2 software was used to analyze the functional effect of missense mutations in genes involved in Hh signaling. PolyPhen-2 provides both a qualitative prediction of inactivation ("damaging" or "benign") and a score.

Description of clinical database, sample preparation, library preparation, bioinformatics processing, flow cytometry analyses, immunoblot analyses, viability assay, and statistical analyses are provided in the supplemental Methods (available on the *Blood* Web site).

Results

Targeted sequencing and Reactome enrichment pathway analysis expands the CLL core pathways list

We performed targeted sequencing of the genes included in the HALT Pan-Leukemia Gene Panel[8] on the CLL cells of 841 treatment-naive patients (Table 1). Of the 103 genes in the HALT Pan-Leukemia Gene Panel, mutations were excluded in 4 genes (*TTN, PCLO, HYDIN,* and *CSMD3*) because they were false-positive findings according to the MutSig algorithm[37] and in 5 genes (*MUC2, MUC4, ASMTL, CRLF2,* and *IL3RA*) that had inadequate coverage criteria (supplemental Table 1). The final list included 94 genes (supplemental Table 2). In 3 of these genes (*CDKN2A, EED,* and *MLH1*), we did not detect mutations in any patient sample. In the remaining 91 genes of the HALT Pan-Leukemia Gene Panel,[8] a total of 1134 variants were identified, 828 (73%) of which involved 84 genes and were considered deleterious (missense, frameshift insertion, frameshift deletion, nonsense, or splicing). A total of 520 of the 841 patients (62%) had one or more deleterious mutations involving one or more of these 84 genes (supplemental Tables 3 and 4). Conversely, 90 patients (11%) had only synonymous mutations, whereas 231 patients (27%) had no detectable mutations in the genes examined. The 5 most commonly mutated genes were *NOTCH1, ATM, TP53, MYD88,* and *SF3B1* (Figure 1; supplemental Figure 1A-C), as noted in previous studies.[1-4,6,38]

Fifty-two (62%) of these 84 genes mapped to the 7 identified CLL signaling/metabolic pathways (supplemental Figure 2). Reactome pathway analysis on the other 32 genes identified significant enrichment of genes implicated in the Hh pathway (false discovery rate = 0.005). Using Cytoscape, we expanded this Reactome pathway analysis to include genes relevant to the Hh pathway from the 84 genes found to have deleterious mutations in our cohort of patients, defining these as *Hh-pathway* genes. These *Hh-pathway* genes included 3 oncogenes (*SMO, GLI1,* and *GLI2*) and 7 additional genes. These 7 additional genes comprised the following: *BCOR* and *BCORL1,* encoding BCL6 corepressor proteins; *CREBBP* and *EP300,* encoding proteins with intrinsic histone acetyl transferase activity; *EZH2,* encoding a protein with histone methyltransferase activity; *FBXW7,* encoding a protein subunit of E3-ubiquitin-protein ligase complex; and *MED12,* encoding mediator complex subunit 12 (Figure 2A-D). A schematic representation of the role of each of the *Hh-pathway* genes found mutated is provided in Figure 2C. The missense mutations found in *SMO* were the first *SMO* mutations identified in CLL, whereas mutations in each of the other 9 genes had been observed in previous studies.[1,4,6,39] Collectively, we identified 102 deleterious mutations in these 10 *Hh-pathway* genes among 89 (11%) of 841 patients examined (Figure 2B).

Patients with CLL who had deleterious mutations in one or more of these 10 *Hh-pathway* genes had a shorter median treatment-free survival (TFS) than patients with CLL cells without *Hh-pathway* mutations (5.4 years vs 6.0 years; $P = .01$). Patients with CLL cells that expressed mutated IGHV (IGHV$_{MU}$) and had mutations in one or more 10 *Hh-pathway* genes had a significantly shorter median TFS than patients with IGHV$_{MU}$ CLL that did not have identified *Hh-pathway* gene mutations (6.4 years vs 9.6 years; $P = .008$) (supplemental Figure 3). Although patients with CLL cells with IGHV$_{UM}$ and mutations identified in

Table 1. Patient characteristics

No. of patients	841
Median age at diagnosis, y (range)	57.2 (30-91)
Sex	
Male	503 (60%)
Female	338 (40%)
Rai stage	
0-1	657 (78%)
2	126 (15%)
3-4	58 (7%)
Median time from diagnosis to Sc, y	3
Median TFS, y	4
No. of treated patients	533 (63%)
No. of patients with IGHV status	830 (98%)
IGHV$_{UM}$	376 (45%)
IGHV$_{MU}$	454 (55%)
No. of patients with ZAP-70 expression	838 (99%)
ZAP-70 positive	307 (37%)
ZAP-70 negative	531 (63%)
No. of patients with fluorescence in situ hybridization data	656 (78%)
Del(17p)	64 (10%)
Del(11q)	78 (12%)
Trisomy 12	103 (16%)
Del(13q)	263 (40%)
Normal karyotype	146 (22%)

Sc, sample collection.

Hh-pathway genes had a median TFS (3.3 years) that seemed shorter than that of patients with IGHV$_{UM}$ CLL cells without identified *Hh-pathway* gene mutations (4.0 years), this difference did not reach statistical significance (*P* = .1, supplemental Figure 3).

GLI1 expression in CLL cells with or without *Hh-pathway* mutations

To evaluate whether mutations in these 10 *Hh-pathway* genes were associated with activation of the Hh pathway, we examined for GLI1 expression in CLL cells from 49 patients randomly selected from the 89 found to have *Hh-pathway* mutations; these selected 49 patients each had CLL cells with one (n = 45) or two (n = 6) deleterious mutations in the 10 *Hh-pathway* genes. Thirty-nine (68%) of the 57 deleterious mutations found among these 49 patient samples were missense mutations. Of these 39 missense mutations, 9 were in oncogenes (*SMO*, *GLI1*, or *GLI2*) and 30 in tumor suppressor genes (*BCOR*, *BCORL1*, *CREBBP*, *EP300*, *FBXW7*, or *MED12*). The PolyPhen-2 prediction software[36] was used to deduce whether any one of these 39 genes would be damaging (Table 2). PolyPhen-2 predicts the possible impact of a missense mutation on the stability and function of human proteins and estimates the probability of a missense mutation being damaging. The PolyPhen-2 score ranges from ≥0.5 to 1.0 for inactivating mutations (damaging) and from 0.0 to <0.5 for not inactivating mutations (benign). According to this approach, 25 (64%) of the 39 identified missense mutations were damaging.

Moreover, we determined that the percentage of missense mutations in tumor suppressor genes that were damaging (62%) was significantly higher than that observed in oncogenes (3%; *P* < .0001) (supplemental Figure 4A-B).

Among these 49 CLL samples with mutations in *Hh-pathway* genes, 41 (84%) expressed GLI1 and hence were classified as GLI1$^+$. Among the cases with missense mutations in *Hh-pathway*–associated oncogenes, all 9 were GLI1$^+$ (Figure 3A), implying that such *Hh-pathway* gene mutations were not inactivating, as predicted according to PolyPhen-2. Consistent with this finding, transfection of CLL cells or U937 cells with either wild-type SMO (SMO$_{WT}$) or P26S mutant SMO (SMO$_{MU}$) increased GLI1 expression (Figure 3B). Among the cases with missense mutations in *Hh-pathway* oncogenes, only 1 had a missense mutation (*GLI2* S941R) that was predicted to be inactivating according to PolyPhen-2 (Table 2). GLI2 and GLI3 transcriptional activator capacity was positively regulated by Hh signaling and negatively regulated by cyclic adenosine monophosphate–dependent protein kinase A (PKA) through specific phosphorylation sites present on GLI2 and GLI3. The inhibition of the formation of full-length GLI2 and GLI3 transcriptional activators (GLI2,3Act) is dependent on all 6 (P1-6) conserved serine residues phosphorylated by PKA. The identified mutation *GLI2* S941R removes the fifth (P5) serine phosphorylation site of PKA.[40] This scenario suggests that this mutation is a gain-of-function mutation that changes GLI2 phosphorylation and consequently affects its ability to induce expression of GLI1. Among the mutations in *Hh-pathway* tumor suppressor genes, 67% were missense, whereas 33% were deleterious mutations other than missense. GLI1 was expressed in 72% of cases with missense mutations and in 94% of deleterious mutations other than missense. We also observed that GLI1 expression was increased when tumor suppressors such as FBXW7, CREBBP, or BCOR were silenced using small interfering RNA (siRNA) in CLL cells lacking GLI1 expression (Figure 3C). None of the 6 cases with benign missense mutations expressed GLI1, whereas all but 2 cases with damaging missense mutations in these tumor suppressor genes expressed GLI1. The 2 cases with CLL cells that carried damaging missense mutations, but lacked GLI1, each had a hotspot FBXW7 mutation (R387C or R479Q) with an allelic fraction <0.20.

We also examined for expression of GLI1 in the CLL cells from 161 patients who randomly were selected from the 752 patients who did not have mutations in any one of the 10 *Hh-pathway* genes. Surprisingly, we found that 62 (38%) of 161 CLL samples without identified *Hh-pathway* gene mutations also expressed GLI1. Although the proportion of cases with identified mutations in the 10 *Hh-pathway* genes that expressed GLI1 (84%) was greater than that noted for cases without mutations in these genes (38%) (χ^2 test, *P* < .0001) (Figure 3D-E), these results reveal that a much larger number of patients in this subcohort (n = 210) have CLL cells with Hh pathway activation (n = 103) than have mutations identified in these 10 *Hh-pathway* genes (n = 49).

Upregulation of GLI1 downstream targets and in vitro response to inhibition of GLI1

We evaluated whether expression of GLI1 correlated with expression of downstream target genes of GLI1, namely *E2F1*, *AKT1*, and *PTCH1*. For this evaluation, CLL cells were randomly collected from 20 Hh$_{MU}$ GLI1$^+$, 8 Hh$_{WT}$ GLI1$^+$, 7 Hh$_{MU}$ GLI1$^-$, and 14 Hh$_{WT}$ GLI1$^-$ patients included in the 210 patients for whom
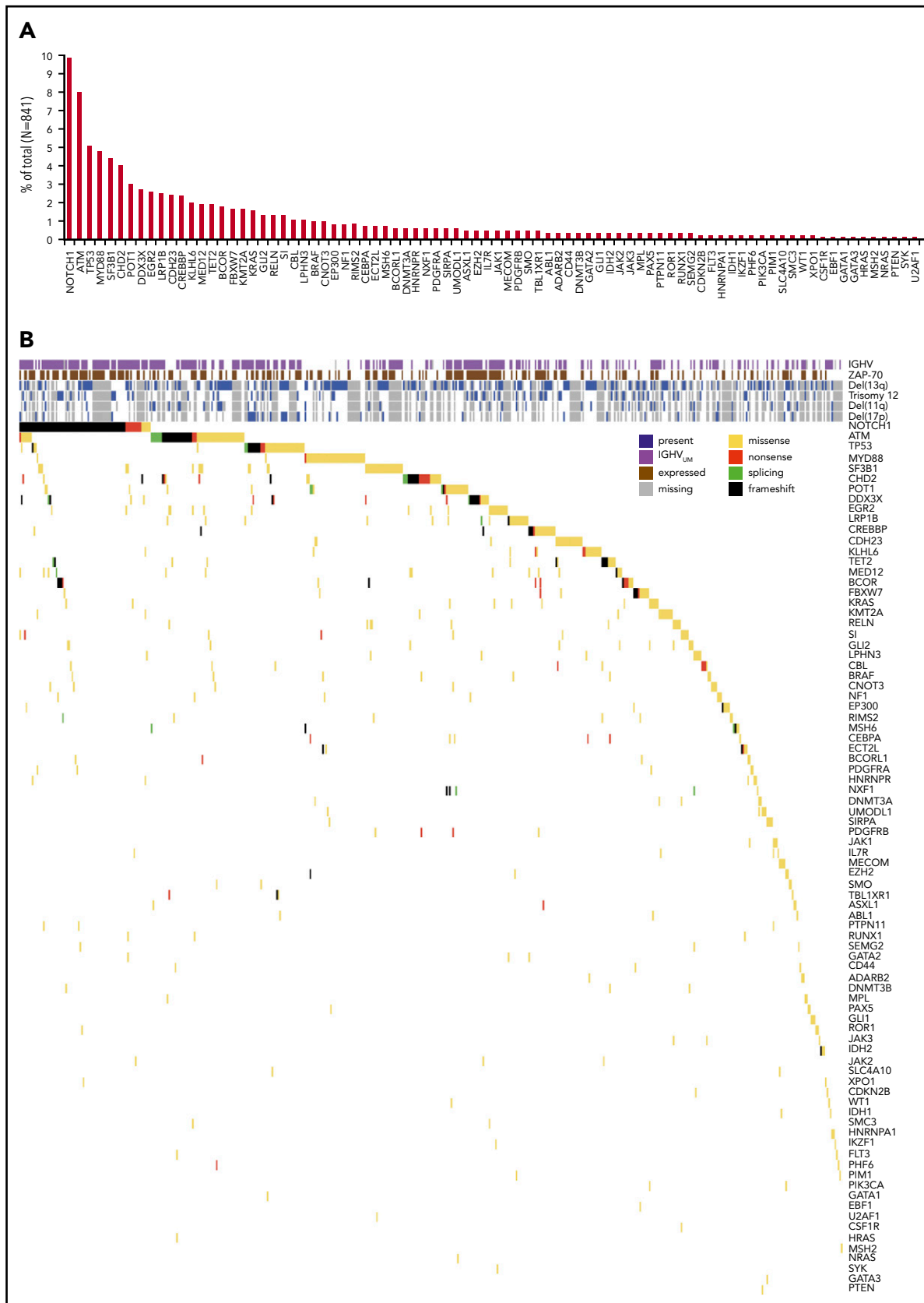
Figure 1. Repertoire of recurrent deleterious mutations observed in 841 patients with CLL. (A) The percentage of cases with mutations in each gene is represented by red bars. (B) Heat map of IGHV mutational status, ZAP-70 expression, cytogenetic aberrations, and deleterious mutations observed in this cohort. Purple boxes indicate which patients have CLL cells with IGHV$_{UM}$, brown boxes indicate which patients have CLL cells expressing ZAP-70, blue boxes indicate which patients have CLL cells carrying cytogenetic deletions (Del13q, Trisomy 12, Del11q, or Del17p), and gray boxes indicate missing data. Yellow boxes represent missense mutations, black frameshift mutations, green splicing mutations, and red nonsense mutations.
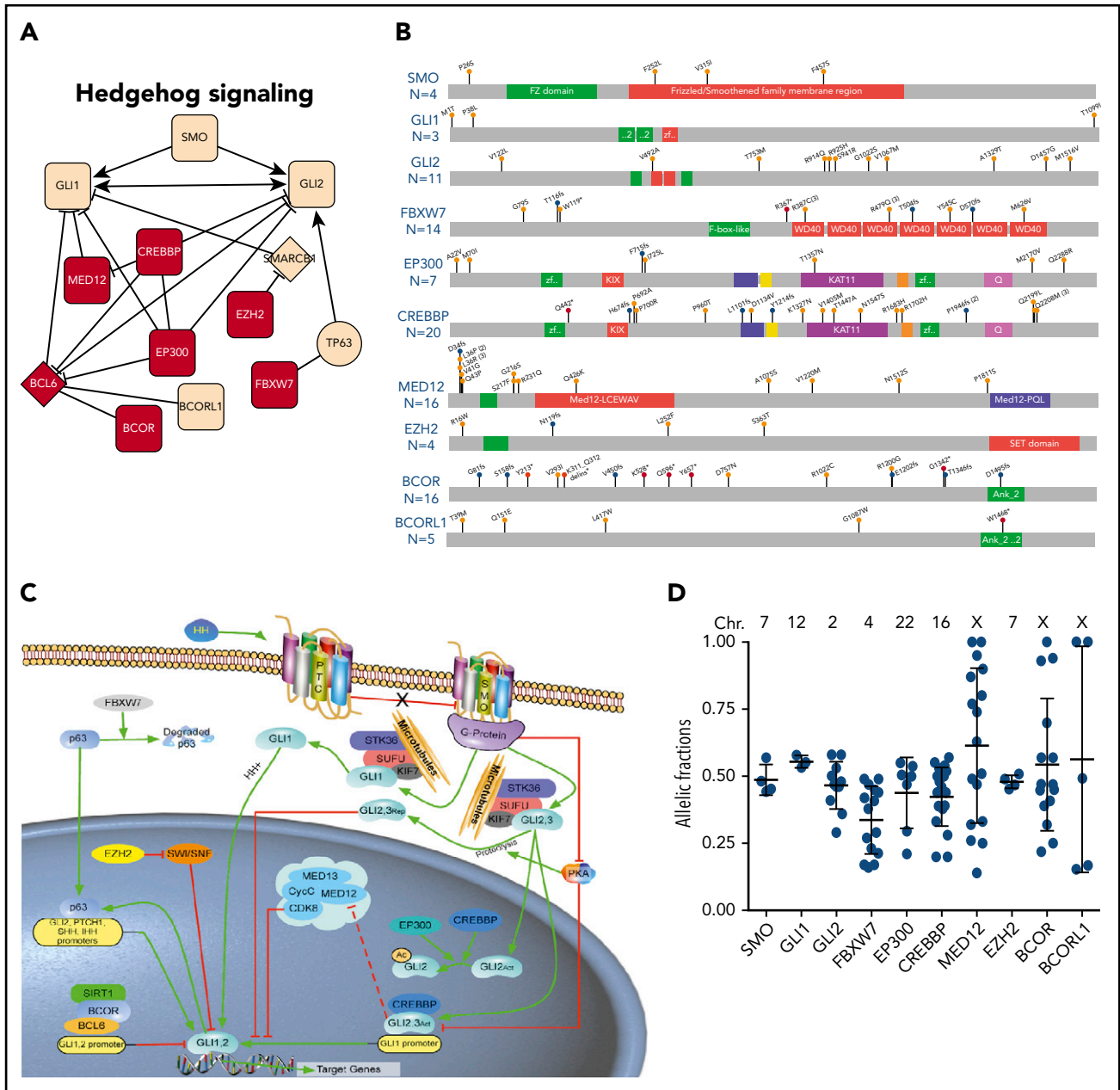
GHIA et al

Figure 2. Hh-pathway genes and their deleterious mutations observed in 841 patients with CLL. (A) Reactome FI Network of Hh signaling pathway identified. Mutated genes (circle shape); genes involved in >1 pathway (red); genes connected but not mutated (diamond shape); and genes found mutated in this study (square shape). Extracted FIs involved in activation, expression regulation, or catalysis are shown with an arrowhead on the end of the line; FIs involved in inhibition are shown with a 'T' bar. (B) Localization and type of 100 deleterious mutations in genes affecting Hh signaling pathway: missense mutations are represented by orange circles, and frameshift and nonsense mutations are represented by blue and red circles, respectively. Two splicing mutations in MED12 and FBXW7 are not included in this figure. Each circle represents a unique mutation; for mutations recurring in >1 individual, the number of individuals is indicated in parentheses. The number of mutations for each gene is indicated below each gene name. (C) Schematic representation of Hh-pathway genes found to be mutated in this cohort as well as in other hematologic diseases. Activation is indicated by green arrows and inhibition by red crossbars. Dashed red crossbar indicates that MED12 inhibition by GLI3 has been reported by Zhou et al[66] while MED12 inhibition by GLI2 is postulated by similarity. The image was modified from Qiagen's original copyrighted image by Emanuela M. Ghia. The original image may be found at https://www.qiagen.com/us/shop/genes-and-pathways/pathway-details/?pwid=220. Please see the Qiagen website for the full terms of use. (D) Allelic fractions of each deleterious mutation observed in Hh-pathway genes are indicated by blue dots. The allelic fraction mean ± standard deviation about the mean, for each gene, are indicated in black. The chromosome location of each gene is indicated above the graph.

GLI1 expression in CLL cells was evaluated. We found that GLI1+ CLL cells had increased E2F1, AKT1, and PTCH1 transcript and protein levels over that of CLL cells lacking expression of GLI1 (Figure 4A-C).

Previous studies showed that BIM is upregulated via an E2F1-dependent mechanism that functions as a prosurvival protein when phosphorylated by AKT at serine 87 ($pBIM_{EL}^{S87}$).[41,42] We found that transcript and protein levels of BIM, as well as $pBIM_{EL}^{S87}$, were significantly upregulated in GLI1+ CLL cells compared with GLI1− CLL cells (Figure 4A-C), showing that expression of GLI1 associates with the activation of downstream targets E2F1 and AKT1, which can upregulate BIM and $pBIM_{EL}^{S87}$ to promote

Table 2. PolyPhen-2 prediction of all missense *Hh-pathway* mutations observed in 49 CLL cases studied for GLI1 expression

Sample ID	Mutated genes	Allelic fraction	Type of mutation	Gene	Mutation	PolyPhen-2 prediction	PolyPhen-2 score
SA00604	*BCOR*	0.47	Missense	*BCOR*	p.R1200G	Benign	0.26
SA00768	*EP300*	0.54	Missense	*EP300*	p.M70I	Benign	0.02
SA00591	*FBXW7*	0.17	Missense	*FBXW7*	p.R387C	Damaging	1.00
SA00952	*FBXW7*	0.17	Missense	*FBXW7*	p.R479Q	Damaging	1.00
SA00499	*FBXW7, EP300*	0.38	Frameshift_deletion	*FBXW7*	p.T504fs		
		0.21	Missense	*EP300*	p.M2170V	Benign	<0.01
SA00732	*MED12, KMT2A*	0.47	Missense	*MED12*	p.Q426K	Benign	0.22
SA00925	*MED12, CHD2*	0.33	Missense	*MED12*	p.G216S	Benign	<0.01
SA01071	*MED12*	1.00	Missense	*MED12*	p.P1811S	Benign	<0.01
SA00455	*MED12, GLI2, CDH23*	0.95	Missense	*MED12*	p.L36R	Damaging	1.00
		0.46	Missense	*GLI2*	p.A1329T	Benign	<0.01
SA00315	*BCOR*	0.57	Nonsense	*BCOR*	p.G1342*		
SA00458	*BCOR, RIMS2, NOTCH1*	0.57	Nonsense	*BCOR*	p.Q596*		
SA00472	*CREBBP*	0.46	Missense	*CREBBP*	p.R1683H	Damaging	0.99
SA00509	*FBXW7, NOTCH1*	0.49	Missense	*FBXW7*	p.R479Q	Damaging	1.00
SA00517	*CREBBP*	0.33	Frameshift_insertion	*CREBBP*	p.P1946fs		
SA00520	*MED12, PTPN11, CHD2, NOTCH1*	0.51	Missense	*MED12*	p.V1220M	Damaging	1.00
SA00556	*CREBBP, ATM, SF3B1*	0.44	Frameshift_deletion	*CREBBP*	p.L1101fs		
SA00578	*CREBBP*	0.50	Missense	*CREBBP*	p.Q2208H	Damaging	0.65
SA00589	*BCORL1, SF3B1, ATM*	0.15	Nonsense	*BCORL1*	p.W1468*		
SA00614	*CREBBP, TP53, NOTCH1*	0.53	Missense	*CREBBP*	p.N1547S	Damaging	0.82
SA00623	*CREBBP, ASXL1*	0.54	Missense	*CREBBP*	p.K1327N	Damaging	0.52
SA00634	*BCOR, KRAS*	0.41	Nonsense	*BCOR*	p.Y213*		
SA00640	*CREBBP*	0.55	Missense	*CREBBP*	p.V1405M	Damaging	0.99
SA00656	*GLI2*	0.53	Missense	*GLI2*	p.S941R	Damaging	1.00
SA00665	*BCOR, CREBBP, KLHL6*	0.39	Missense	*CREBBP*	p.T1447A	Damaging	0.97
		0.94	Nonsense	*BCOR*	p.Y657*		
SA00695	*MED12, GLI2*	0.25	Missense	*MED12*	p.S217F	Damaging	0.76
		0.58	Missense	*GLI2*	p.D1457G	benign	0.01
SA00356	*GLI1*	0.58	Missense	*GLI1*	p.P38L	benign	<0.01
SA00784	*CREBBP, MED12, PDGFRB*	0.38	Missense	*CREBBP*	p.P960T	Damaging	1.00
		0.63	Missense	*MED12*	p.L36R	Damaging	1.00
SA00803	*BCOR, NOTCH1, NF1*	0.32	Frameshift_deletion	*BCOR*	p.G81fs		
SA00846	*EP300*	0.50	Missense	*EP300*	p.A22V	Damaging	0.94

Table 2. (continued)

Sample ID	Mutated genes	Allelic fraction	Type of mutation	Gene	Mutation	PolyPhen-2 prediction	PolyPhen-2 score
SA00847	MED12, ATM, LRP1B	0.32	Missense	MED12	p.L36R	Damaging	1.00
		0.26	Missense	MED12	p.V41G	Damaging	0.97
SA00366	FBXW7	0.29	Missense	FBXW7	p.R387C	Damaging	1.00
SA00889	MED12, CHD2, ATM	0.90	Missense	MED12	p.Q43P	Damaging	0.93
SA00894	CREBBP	0.39	Missense	CREBBP	p.P700R	Damaging	0.73
SA00902	CREBBP	0.44	Missense	CREBBP	p.Q2208H	Damaging	0.65
SA00948	BCOR	0.47	Frameshift_deletion	BCOR	p.D1495fs		
SA00959	GLI2, NOTCH1	0.36	Missense	GLI2	p.R925H	Benign	<0.01
SA01000	FBXW7	0.27	Frameshift_deletion	FBXW7	p.T116fs		
SA01014	BCOR	1.00	Nonsense	BCOR	p.K528*		
SA01015	FBXW7, CD44	0.41	Frameshift_insertion	FBXW7	p.D570fs		
SA01042	GLI2, JAK3, RELN	0.47	Missense	GLI2	p.V122L	Benign	0.03
SA01043	SMO	0.48	Missense	SMO	p.P26S	Benign	0.02
SA01066	GLI2, DNMT3B	0.48	Missense	GLI2	p.M1516V	Benign	0.29
SA01089	GLI2, NOTCH1	0.29	Missense	GLI2	p.T753M	Benign	0.23
SA01094	BCOR, SF3B1	0.25	Frameshift_deletion	BCOR	p.E1202fs		
SA01129	FBXW7	0.45	Missense	FBXW7	p.R479Q	Damaging	1.00
SA01138	BCOR, NOTCH1	0.93	Frameshift_deletion	BCOR	p.V450fs		
SA00392	BCORL1, NOTCH1	1.00	Missense	BCORL1	p.T39M	Damaging	0.61
SA00308	FBXW7	0.42	Nonsense	FBXW7	p.W119*		
SA00313	MED12, CREBBP, GATA2	0.77	Missense	MED12	p.L36P	Damaging	1.00
		0.20	Frameshift_insertion	CREBBP	p.P1946fs		

cell survival (Figure 4D). Consistent with this finding, a significant reduction was observed in the viability of GLI1$^+$ CLL cells when GLI1 was silenced by using GLI1-specific siRNA but not nonspecific siRNA ($P < .0001$) (Figure 4E-F; supplemental Figure 5).

We evaluated the sensitivity of GLI1$^+$ or GLI1$^-$ CLL cells to GANT61, a small molecule inhibitor of GLI1. GLI1$^+$ CLL cells were significantly more sensitive to treatment with GANT61 than GLI1$^-$ CLL cells regardless of whether they had mutations identified in the 10 Hh-pathway genes ($P < .001$) (Figure 4G). In addition, GANT61 treatment reduced the protein level of BIM and the phosphorylation level of pBIM$_{EL}$^{S87} in GLI1$^+$ CLL cells (Figure 4H).

GLI1 expression is associated with disease progression

The median TFS of patients with CLL cells that were GLI1$^+$ (n = 103) was compared with that of patients who had CLL cells that were GLI1$^-$ (n = 107). Cases with GLI1$^+$ CLL cells had a significantly shorter median TFS compared with patients with

GLI1$^-$ CLL (4.7 years vs 6.4 years; $P = .002$) (Figure 5A). Expression of GLI1 was associated with more rapid disease progression independent of identified mutations in the 10 Hh-pathway genes (supplemental Figure 6). Moreover, GLI1 expression was associated with significantly shorter median TFS, independent of IGHV mutational status (5.3 years vs 9.8 years [$P = .003$] for patients with CLL with IGHV$_{MU}$ and 3.3 years vs 4.4 years [$P = .02$] for patients with CLL cells with IGHV$_{UM}$) (Figure 5B).

Discussion

The current study found that mutations in one or more genes involved in Hh signaling were not uncommon in CLL. This report is the first to indicate that CLL cells may harbor mutations in SMO, a Frizzled G protein–coupled receptor for Hh ligands. Moreover, we identified mutations in other genes encoding proteins that may govern activation of the Hh pathway, namely GLI1, GLI2, BCOR, BCORL1, CREBBP, EP300, EZH2, FBXW7, and MED12, which other studies had identified as harboring mutations in CLL but had not been collectively identified as

Figure 3. Relationship between GLI1 expression and *Hh-pathway* mutations. (A) GLI1 protein expression in CLL cells with missense mutations (n = 39) deduced as being benign or damaging according to PolyPhen-2. The horizontal bar in each group provides the mean level of GLI1 protein expression observed for each group. The Mann-Whitney *U* test was used to calculate the *P* value indicated at the top. (B) Immunoblot analyses of CLL cells and the U937 cell line transfected with empty vector (C–), wild-type SMO (SMO_WT_), or mutant SMO carrying P26S, which is a non-inactivating missense mutation (SMO_MU_), as indicated at the top. The membranes were probed with a monoclonal antibody mAb specific for GLI1, SMO, or β-actin as indicated on the left margin. The expression of β-actin was used to normalize GLI1 and SMO expression. The ratios of the band densities are provided at the bottom of each blot. (C) Immunoblot analyses for proteins indicated on the right using lysates of CLL cells that were treated with control siRNA (siCTR) or tumor suppressor–specific (siFBXW7 or siCREBBP or siBCOR) siRNA as indicated. (D) Densitometry analysis of immunoblot in panel E quantifying GLI1 protein expression levels for CLL sample with leukemia cells with or without *Hh-pathway* mutations (Hh_MU_, n = 49; Hh_WT_, n = 161). The horizontal bar in each group provides the mean level of GLI1 protein expression observed for each group. The Mann-Whitney *U* test was used to calculate the *P* value indicated at the top. (E) Immunoblot analyses of CLL cells with or without *Hh-pathway* mutations (Hh_MU_), as indicated at the top. Each lane represents a separate case. The membranes were probed with a monoclonal antibody specific for GLI1 or β-actin, as indicated on the left margin. The density of the β-actin band was used to normalize band density for GLI1 in each sample. The ratios of the band densities of GLI1/β-actin for each sample are indicated at the bottom and presented in the dot-plots in panel D. The same protein lysate from JeKo-1 cells was used as a positive control (C+) in all gels. GLI1⁺ CLL samples were defined as those with ratios of the band densities of GLI1/β-actin >0.1.

Figure 4. Relationship between GLI1 expression and GLI1 downstream targets. (A) *GLI1, PTCH1, E2F1, AKT1,* and *BIM* transcript levels in CLL cells expressing or lacking GLI1 (GLI1+, n = 28; GLI1−, n = 21). The Mann-Whitney *U* test was used to calculate the *P* value indicated at the top. (B) Representative immunoblot analyses of CLL cells with or without GLI1 expression (GLI1+, n = 28; GLI1−, n = 21), as indicated at the top. Each lane represents a separate case. The membranes were probed with a monoclonal antibody specific for GLI1, PTCH1, E2F1, AKT1, pBIM, and BIM or β-actin as indicated on the left margin. The expression of β-actin was used to normalized GLI1, PTCH1, E2F1, AKT1, and BIM expression levels. The ratios of the band densities for each case are provided at the bottom of each blot and presented in the dot-plots in panel C. The ratios of the band densities for each case of $pBIM_{EL}^{S87}/BIM_{EL}$ is indicated at the bottom of the $pBIM_{EL}^{S87}$ blot and represented in the dot-plots in panel C. The same GLI1+ CLL protein lysate sample was used as positive control in all gels. (C) Densitometry analysis quantifying the protein expression levels of GLI1 and its downstream targets in all 49 cases with CLL cells with or without GLI1 expression. The horizontal bar provides the mean ratio observed in each group. The Mann-Whitney *U* test was used to calculate the *P* value indicated at the top. (D) Schematic representation of the consequences of GLI1 upregulation on its downstream targets. (E) Relative viability of CLL cells treated with control siRNA (siCTR) or GLI1-specific siRNA (siGLI1) as indicated. (F) Immunoblot analyses for GLI1 using lysates of CLL cells expressing GLI1 treated with siCTR or siGLI1. Data from 2 representative patients are presented. (G) Relative viability of CLL cells expressing GLI1 with (GLI1+ Hh_{MU}, n = 6; red squares) or without (GLI1+ Hh_{WT} N = 3, gray squares) Hh mutations or lacking GLI1 expression with (GLI1− Hh_{MU}, n = 3; blue circles) or without (GLI1− Hh_{WT}, n = 6; yellow circles) Hh mutations treated for 24 hours with 5 or 10 μM of GANT61. Data are shown as mean ± standard deviation. (H) Immunoblot analyses of CLL cells expressing GLI1 and treated for 24 hours with 10 μM of GANT61. The membranes were probed with a monoclonal antibody specific for GLI1, pBIM, and BIM or β-actin as indicated on the left margin. The expression of β-actin was used to normalized GLI1 and BIM expression level. The ratios of the band densities for each case are provided at the bottom of each blot. The ratios of the band densities for each case of $pBIM_{EL}^{S87}/BIM_{EL}$ are indicated at the bottom of the $pBIM_{EL}^{S87}$ blot. Data from 2 representative patients are presented.
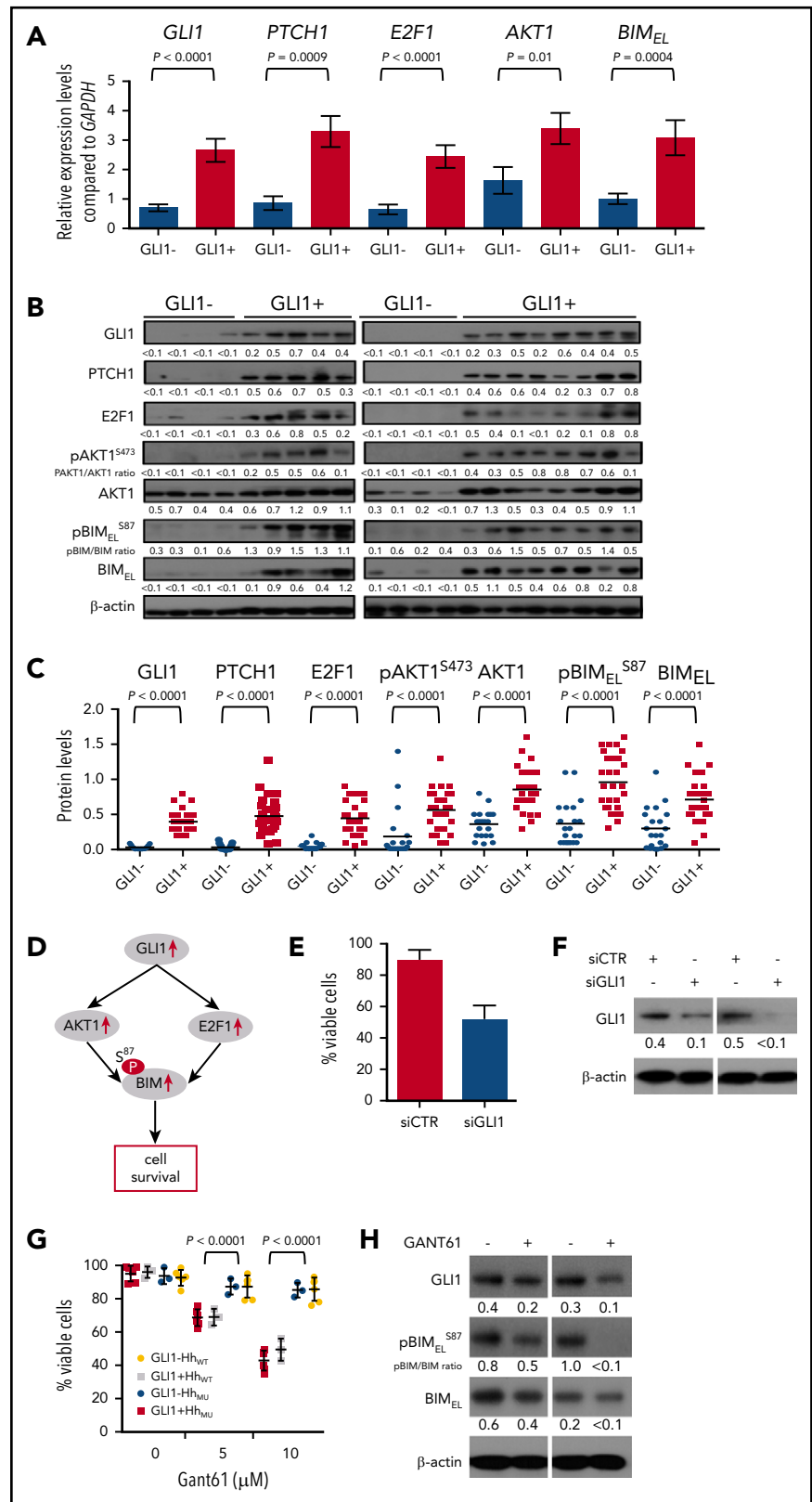
being involved in Hh signaling.[1,4,6,39] We found that the leukemia cells of 89 (11%) patients among the 841 treatment-naive patients studied had nonsynonymous mutations in one or more of these *Hh-pathway* genes.

Some of the mutations identified in this study are directly involved in Hh signaling. The missense mutation (P26S) identified in *SMO* causes a proline→serine substitution, which was not predicted to inactivate its function but rather enhance its
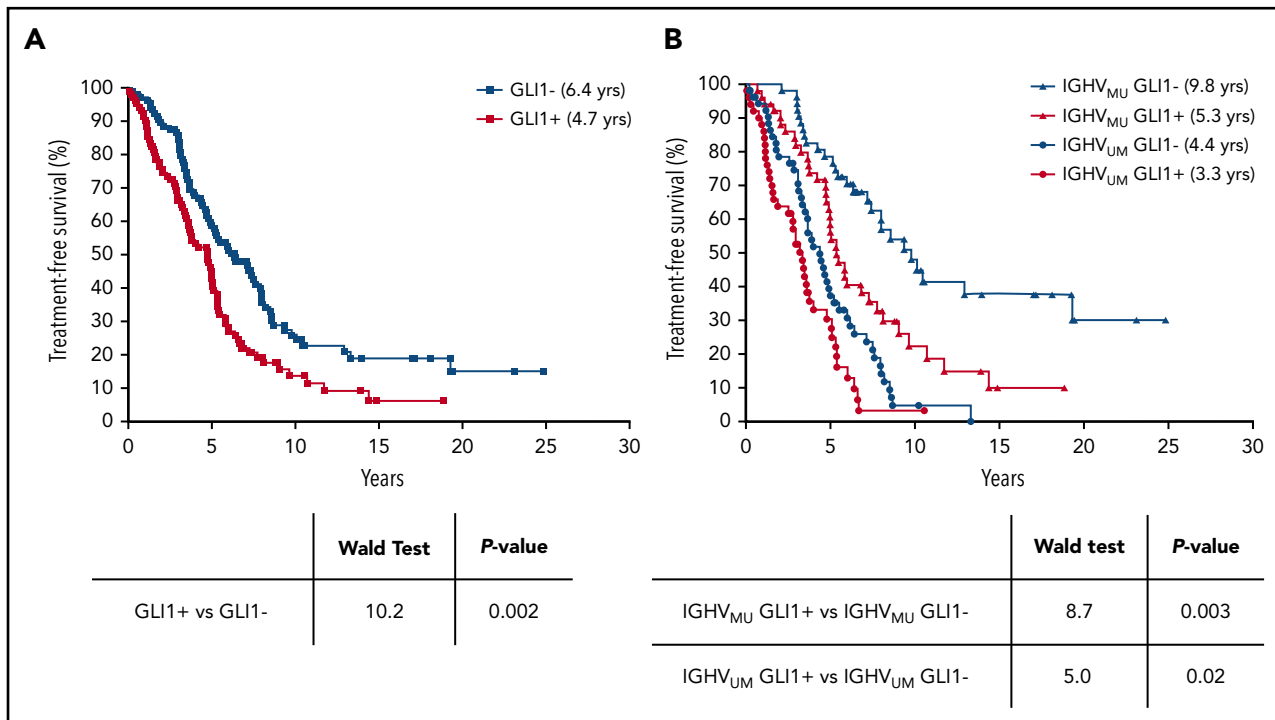
Figure 5. Relationship between GLI1 expression and TFS. (A) Kaplan-Meier curves depict the TFS probability over time for GLI1^{+} (red squares) or GLI1^{−} (blue squares) CLL (N = 210). (B) Kaplan-Meier curves depict the TFS probability over time for IGHV$_{UM}$ GLI1^{+} (red circles), IGHV$_{UM}$ GLI1^{−} (blue circles), IGHV$_{MU}$ GLI1^{+} (red triangles), or IGHV$_{MU}$ GLI1^{−} (blue triangles) subgroups of all patients with CLL and known IGHV status for whom GLI1 expression was evaluated (N = 206).

capacity to activate Hh signaling. Consistent with this finding, we observed that CLL cells or U937 cells transfected with either SMO$_{WT}$ or SMO$_{MU}$ (P26S) increased expression of GLI1, arguing that the identified mutant *SMO* encoded a functional protein. This scenario contrasts with other *SMO* mutants, which encode proteins that cannot undergo the serine phosphorylation and/or cell surface accumulation that are required to activate Hh signaling.[43-45] Instead, the SMO mutation we identified in CLL seems similar to the missense *SMO* mutations found to be associated with Hh pathway activation in solid tumors,[13,46,47] T-cell acute lymphoblastic leukemia (T-ALL),[48] or basal cell skin carcinomas.[14] We also identified 1 case with CLL cells carrying a missense mutation in *GLI2*, causing a serine→arginine substitution at position 941, which previous studies showed affected GLI2 phosphorylation and enhanced its capacity to induce GLI1.[40,49] Consistent with this outcome, we found that CLL cells harboring this mutation expressed high levels of GLI1.

We also found that 14 of the 841 study patients had CLL cells harboring mutations in *FBXW7*. FBXW7 encodes an F-box factor that targets selected proteins for ubiquitin-mediated degradation.[50] *FBXW7* is mutated in a wide spectrum of human cancers,[51] where it acts as a tumor suppressor. Moreover, studies have identified numerous mutations in *FBXW7* and/or its substrates in cancer cells and found that loss of FBXW7 function associates with chromosomal instability and tumorigenesis.[52,53] The *FBXW7* mutations that we and others have identified in CLL, or ALL,[1,54,55] result in substitutions within the WD40 domain required for targeting the destruction of selected proteins,[51,56,57] such as p63,[58] which can induce activation of the Hh pathway.[59] In the current study, siRNA-mediated silencing of *FBXW7* in CLL cells expressing wild-type *FBXW7* enhanced the expression of GLI1,

indicating that FBXW7 serves to suppress Hh pathway activation in this leukemia. Consistent with the notion that the deleterious mutations we identified in *FBXW7* can lead to activation of Hh signaling, we observed that 70% of cases with CLL cells harboring *FBXW7* mutations overexpressed GLI1. These *FBXW7* mutations associated with GLI1 expression almost invariably were present at allelic fractions of >20%, arguing that such mutations may be conducive to subclonal disease progression. Selective growth advantage for subclones with Hh activation due to deleterious mutations in *FBXW7* could contribute to outgrowth of subclones harboring mutations in *FBXW7* and *BTK* or *PLCG2* in leukemia cells of patients who develop resistance to inhibitors of Bruton tyrosine kinase such as ibrutinib.[60,61]

Fifteen cases with CLL cells harboring mutations in *BCOR* were also identified. BCOR is a BCL6 transcriptional corepressor that can complex with BCL6 to recruit HDAC3-containing SMRT complexes that repress transcription of selected genes,[62] such as *GLI1* and *GLI2*, which are critical for Hh pathway activation.[63] In the current study, down-modulation of *BCOR* using specific siRNA in primary CLL cells that expressed wild-type *BCOR* increased expression of GLI1, indicating that BCOR may serve to repress Hh pathway activation in this leukemia. Although nonsynonymous mutations in *BCOR* can affect its ability to repress transcription,[64] we noted that 75% of the observed *BCOR* mutations were either nonsense or frameshift mutations, which would be expected to abrogate BCOR expression, thus impairing their capacity to repress Hh pathway activation. Consistent with this notion, high levels of GLI1 were expressed by all but one of the CLL samples with a mutation in *BCOR*; the one sample that did not express high levels of GLI1 had a benign missense mutation in *BCOR* that is not expected to affect function. As with

FBXW7, selective growth advantage for subclones with Hh activation due to deleterious mutations in *BCOR* could contribute to outgrowth of subclones harboring mutations in *BCOR* and *BTK* in leukemia cells of patients who develop resistance to ibrutinib.[60]

We also identified 27 CLL samples in the 841 examined that had damaging mutations in *CREBBP* (n = 20) or *EP300* (n = 7) that would be expected to impair expression and/or function. EP300/CREBBP family members can acetylate GLI2 at lysine 757 and thereby inhibit its capacity to induce expression of *GLI1* and Hh target genes.[65] In the current study, down-modulation of *CREBBP* in primary CLL cells with specific siRNA increased expression of GLI1, indicating that *CREBBP* may serve to repress Hh pathway activation in this leukemia. Consistent with this notion, GLI1 was reportedly overexpressed in all CLL cells harboring *CREBBP* mutations.

Finally, we identified 16 samples in the 841 samples examined that had mutations in *MED12*, encoding Mediator complex subunit 12 (MED12), which can be targeted by activated GLI3 to reverse suppression of Hh target gene transcription.[66] GLI3-dependent Hh signal transduction is negatively modulated by MED12 by anchoring CDK8 in the Mediator of the preinitiation gene-transcriptional complex. A previous study by Kämpjärvi et al[67] screened >700 CLL samples for *MED12* mutations in exons 1 and 2 and found that 10% of all *MED12* mutations occurred within mutation hotspots (codons L36 and Q43). Mutations within exons 1 and 2 were previously reported to share similar gene expression profiles; functional analyses indicated that these mutations contributed to the decrease of Mediator-associated kinase activity.[68,69] Of the 16 cases of *MED12* mutations identified in the current study, one half were located in exon 2 and 37% were in L36 or Q43 hotspots; such mutations would be anticipated to impair function. Consistent with this notion, we found that CLL cells harboring *MED12* mutations almost invariably had high-level expression of GLI1. Exceptions to this were noted in 3 cases that had *MED12* mutations outside exon 2 that were predicted to not affect function; none of these cases expressed GLI1.

Although we found that a significantly higher proportion of the CLL cases with mutations in *Hh-pathway* genes expressed GLI1 than CLL without such mutations, a major finding of this study was that an unexpectedly large number of cases without identified Hh pathway mutations were GLI1+. Although 84% of patients with CLL cells with mutations in the 10 *Hh-pathway* genes overexpressed GLI1, we discovered that more than one third (38%) of samples lacking identified mutations also expressed high levels of GLI1. As such, nearly one half (49%) of the subcohort of 210 CLL cases examined had activation of the Hh pathway.

The finding that a high proportion of CLL cells express GLI1 has apparent functional and clinical significance. We found that expression of GLI1 was associated with significant increases in the transcript and protein levels of downstream targets of GLI1, namely E2F1 and AKT1, which were associated with increased expression and phosphorylation, respectively, of BIM. Furthermore, patients with GLI1+ CLL cells were observed to have a significantly shorter median TFS than patients with GLI1− CLL cells independent of IGHV mutation status. The finding that the expression of GLI1 could segregate even those patients with CLL cells that used unmutated IGHV into subgroups with significantly

different median TFS implies that activation of the Hh pathway can strongly influence disease progression in CLL, as has been noted in other cancers.[18-21]

Human lymphoid malignancies, such as T-ALL,[70] diffuse large B-cell lymphoma,[71] anaplastic large cell lymphoma driven by nucleophosmin-anaplastic lymphoma kinase,[72] mantle cell lymphoma,[73] or multiple myeloma,[24,74] have been shown to have frequent activation of the Hh signaling pathway and sensitivity to SMO and GLI1 inhibitors. In this study, we found that GLI1+ CLL cells were significantly more sensitive to treatment with GANT61 than GLI1− CLL cells, regardless of whether the CLL cells had mutations in any 1 of the 10 *Hh-pathway* genes. This outcome suggests that the survival of GLI1+ CLL cells may have a greater dependency on activation of the Hh pathway. Activation of this pathway apparently may result from mutations in genes encoding proteins downstream of SMO, making cells harboring such mutations potentially insensitive to agents that solely inhibit SMO. Such cells still would be expected to be sensitive to inhibition of GLI1, which is a primary effector of Hh signaling. Finding frequent mutations in genes associated with the Hh pathway downstream of SMO could account for the relatively low activity of SMO inhibitors compared with GLI1 inhibitors in killing CLL cells in vitro.[27,28,30]

Nonetheless, the current study identified that a high proportion of the patients have CLL cells that have activation of the Hh pathway. Agents that block expression or function of GLI may be particularly active in such patients. Targeting GLI1 could block ligand-independent and ligand-dependent Hh pathway activation and perhaps overcome the apparent resistance to SMO inhibitors. As such, this report shows that the Hh pathway frequently is activated in CLL and associated with relatively rapid disease progression, while identifying a new avenue for therapeutic intervention for patients with this disease.

Authorship

Contribution: E.M.G. and L.Z.R. designed, performed the research, analyzed the data, and wrote the paper; F.Y., J.D.M., and T.J.H. generated the

Correspondence: Thomas J. Kipps, Moores Cancer Center, University of California San Diego, 3855 Health Sciences Dr, Room 4307, San Diego, CA 92093-0820; e-mail: tkipps@ucsd.edu.

Footnotes

REFERENCES

1. Landau DA, Carter SL, Stojanov P, et al. Evolution and impact of subclonal mutations in chronic lymphocytic leukemia. *Cell*. 2013; 152(4):714-726.

2. Landau DA, Tausch E, Taylor-Weiner AN, et al. Mutations driving CLL and their evolution in progression and relapse. *Nature*. 2015; 526(7574):525-530.

3. Puente XS, Beà S, Valdés-Mas R, et al. Noncoding recurrent mutations in chronic lymphocytic leukaemia. *Nature*. 2015;526(7574): 519-524.

4. Quesada V, Conde L, Villamor N, et al. Exome sequencing identifies recurrent mutations of the splicing factor SF3B1 gene in chronic lymphocytic leukemia. *Nat Genet*. 2011;44(1): 47-52.

5. Smith EN, Ghia EM, DeBoever CM, et al. Genetic and epigenetic profiling of CLL disease progression reveals limited somatic evolution and suggests a relationship to memory-cell development. *Blood Cancer J*. 2015;5(4):e303.

6. Wang L, Lawrence MS, Wan Y, et al. SF3B1 and other novel cancer genes in chronic lymphocytic leukemia. *N Engl J Med*. 2011; 365(26):2497-2506.

7. Kipps TJ, Stevenson FK, Wu CJ, et al. Chronic lymphocytic leukaemia. *Nat Rev Dis Primers*. 2017;3:16096.

8. Shlush LI, Zandi S, Mitchell A, et al; HALT Pan-Leukemia Gene Panel Consortium. Identification of pre-leukaemic haematopoietic stem cells in acute leukaemia [published correction appears in *Nature*. 2014;508(7496):420]. *Nature*. 2014; 506(7488):328-333.

9. Haw R, Hermjakob H, D'Eustachio P, Stein L. Reactome pathway analysis to enrich biological discovery in proteomics data sets. *Proteomics*. 2011;11(18):3598-3613.

10. Chung JH, Bunz F. A loss-of-function mutation in PTCH1 suggests a role for autocrine hedgehog signaling in colorectal tumorigenesis. *Oncotarget*. 2013;4(12):2208-2211.

11. Mar BG, Amakye D, Aifantis I, Buonamici S. The controversial role of the Hedgehog pathway in normal and malignant hematopoiesis. *Leukemia*. 2011;25(11):1665-1673.

12. Sheng T, Li C, Zhang X, et al. Activation of the hedgehog pathway in advanced prostate cancer. *Mol Cancer*. 2004;3(1):29.

13. Wang XD, Inzunza H, Chang H, et al. Mutations in the hedgehog pathway genes SMO and PTCH1 in human gastric tumors. *PLoS One*. 2013;8(1):e54415.

14. Xie J, Murone M, Luoh SM, et al. Activating Smoothened mutations in sporadic basal-cell carcinoma. *Nature*. 1998;391(6662):90-92.

15. Liu Z, Xu J, He J, et al. A critical role of autocrine sonic hedgehog signaling in human CD138+ myeloma cell survival and drug resistance. *Blood*. 2014;124(13):2061-2071.

16. Shou Y, Robinson DM, Amakye DD, et al. A five-gene hedgehog signature developed as a patient preselection tool for hedgehog inhibitor therapy in medulloblastoma. *Clin Cancer Res*. 2015;21(3):585-593.

17. Hu M, Hong J, Zhang J. Clinical value of glioma-associated oncogene homolog 1 as a prognostic marker in cancer: a meta-analysis. *Int J Clin Exp Med*. 2016;9(12):23008-23018.

18. Zahreddine HA, Culjkovic-Kraljacic B, Assouline S, et al. The sonic hedgehog factor GLI1 imparts drug resistance through inducible glucuronidation. *Nature*. 2014; 511(7507):90-93.

19. ten Haaf A, Bektas N, von Serenyi S, et al. Expression of the glioma-associated oncogene homolog (GLI) 1 in human breast cancer is associated with unfavourable overall survival. *BMC Cancer*. 2009;9(1):298.

20. Liao X, Siu MK, Au CW, et al. Aberrant activation of hedgehog signaling pathway in ovarian cancers: effect on prognosis, cell invasion and differentiation. *Carcinogenesis*. 2009;30(1):131-140.

21. Bora-Singhal N, Perumal D, Nguyen J, Chellappan S. Gli1-mediated regulation of Sox2 facilitates self-renewal of stem-like cells and confers resistance to EGFR inhibitors in non-small cell lung cancer. *Neoplasia*. 2015; 17(7):538-551.

22. Miele E, Po A, Begalli F, et al. β-arrestin1-mediated acetylation of Gli1 regulates Hedgehog/Gli signaling and modulates self-renewal of SHH medulloblastoma cancer stem cells. *BMC Cancer*. 2017;17(1):488.

23. Nayak A, Satapathy SR, Das D, et al. Nanoquinacrine induced apoptosis in cervical cancer stem cells through the inhibition of hedgehog-GLI1 cascade: role of GLI-1. *Sci Rep*. 2016;6(1):20600.

24. Peacock CD, Wang Q, Gesell GS, et al. Hedgehog signaling maintains a tumor stem cell compartment in multiple myeloma. *Proc Natl Acad Sci U S A*. 2007;104(10):4048-4053.

25. Tanaka H, Nakamura M, Kameda C, et al. The Hedgehog signaling pathway plays an essential role in maintaining the CD44+CD24-/low subpopulation and the side population of breast cancer cells. *Anticancer Res*. 2009; 29(6):2147-2157.

26. Zhao C, Chen A, Jamieson CH, et al. Hedgehog signalling is essential for maintenance of cancer stem cells in myeloid leukaemia [published correction appears in *Nature*. 2009;460(7255):652]. *Nature*. 2009; 458(7239):776-779.

27. Decker S, Zirlik K, Djebatchie L, et al. Trisomy 12 and elevated GLI1 and PTCH1 transcript levels are biomarkers for Hedgehog-inhibitor responsiveness in CLL. *Blood*. 2012;119(4): 997-1007.

28. Desch P, Asslaber D, Kern D, et al. Inhibition of GLI, but not Smoothened, induces apoptosis in chronic lymphocytic leukemia cells. *Oncogene*. 2010;29(35):4885-4895.

29. Hegde GV, Peterson KJ, Emanuel K, et al. Hedgehog-induced survival of B-cell chronic lymphocytic leukemia cells in a stromal cell microenvironment: a potential new therapeutic target. *Mol Cancer Res*. 2008;6(12): 1928-1936.

30. Kern D, Regl G, Hofbauer SW, et al. Hedgehog/ GLI and PI3K signaling in the initiation and maintenance of chronic lymphocytic leukemia. *Oncogene*. 2015;34(42):5341-5351.

31. Hallek M, Cheson BD, Catovsky D, et al; International Workshop on Chronic Lymphocytic Leukemia. Guidelines for the diagnosis and treatment of chronic lymphocytic leukemia: a report from the International Workshop on Chronic Lymphocytic Leukemia updating the National Cancer Institute-Working Group 1996 guidelines. *Blood*. 2008;111(12):5446-5456.

32. Shannon P, Markiel A, Ozier O, et al. Cytoscape: a software environment for integrated models of

biomolecular interaction networks. *Genome Res.* 2003;13(11):2498-2504.

33. Wu G, Dawson E, Duong A, Haw R, Stein L. ReactomeFIViz: a Cytoscape app for pathway and network-based data analysis. *F1000 Res.* 2014;3:146.

34. Wu G, Feng X, Stein L. A human functional protein interaction network and its application to cancer data analysis. *Genome Biol.* 2010; 11(5):R53.

35. Croft D, Mundo AF, Haw R, et al. The Reactome pathway knowledgebase. *Nucleic Acids Res.* 2014;42(Database issue):D472-D477.

36. Adzhubei IA, Schmidt S, Peshkin L, et al. A method and server for predicting damaging missense mutations. *Nat Methods.* 2010;7(4): 248-249.

37. Lawrence MS, Stojanov P, Polak P, et al. Mutational heterogeneity in cancer and the search for new cancer-associated genes. *Nature.* 2013;499(7457):214-218.

38. Puente XS, Pinyol M, Quesada V, et al. Whole-genome sequencing identifies recurrent mutations in chronic lymphocytic leukaemia. *Nature.* 2011;475(7354):101-105.

39. Takahashi K, Hu B, Wang F, et al. Clinical implications of cancer gene mutations in patients with chronic lymphocytic leukemia treated with lenalidomide. *Blood.* 2018; 131(16):1820-1832.

40. Niewiadomski P, Kong JH, Ahrends R, et al. Gli protein activity is controlled by multisite phosphorylation in vertebrate Hedgehog signaling. *Cell Reports.* 2014;6(1):168-181.

41. Gogada R, Yadav N, Liu J, et al. Bim, a proapoptotic protein, up-regulated via transcription factor E2F1-dependent mechanism, functions as a prosurvival molecule in cancer. *J Biol Chem.* 2013;288(1):368-381.

42. Qi XJ, Wildey GM, Howe PH. Evidence that Ser87 of BimEL is phosphorylated by Akt and regulates BimEL apoptotic function. *J Biol Chem.* 2006;281(2):813-823.

43. Chen Y, Sasai N, Ma G, et al. Sonic Hedgehog dependent phosphorylation by CK1α and GRK2 is required for ciliary accumulation and activation of smoothened. *PLoS Biol.* 2011; 9(6):e1001083.

44. Jia J, Tong C, Wang B, Luo L, Jiang J. Hedgehog signalling activity of Smoothened requires phosphorylation by protein kinase A and casein kinase I. *Nature.* 2004;432(7020): 1045-1050.

45. Zhao Y, Tong C, Jiang J. Hedgehog regulates smoothened activity by inducing a conformational switch. *Nature.* 2007;450(7167): 252-258.

46. Kool M, Jones DT, Jäger N, et al; ICGC PedBrain Tumor Project. Genome sequencing of SHH medulloblastoma predicts genotype-related response to smoothened inhibition. *Cancer Cell.* 2014;25(3):393-405.

47. Sicklick JK, Li YX, Jayaraman A, et al. Dysregulation of the Hedgehog pathway

in human hepatocarcinogenesis. *Carcinogenesis.* 2006;27(4):748-757.

48. Dagklis A, Pauwels D, Lahortiga I, et al. Hedgehog pathway mutations in T-cell acute lymphoblastic leukemia. *Haematologica.* 2015;100(3):e102-e105.

49. Pan Y, Wang C, Wang B. Phosphorylation of Gli2 by protein kinase A is required for Gli2 processing and degradation and the Sonic Hedgehog-regulated mouse development. *Dev Biol.* 2009;326(1):177-189.

50. Randle SJ, Laman H. F-box protein interactions with the hallmark pathways in cancer. *Semin Cancer Biol.* 2016;36:3-17.

51. Akhoondi S, Sun D, von der Lehr N, et al. FBXW7/hCDC4 is a general tumor suppressor in human cancer [published correction appears in *Cancer Res.* 2008;68(4):1245]. *Cancer Res.* 2007;67(19):9006-9012.

52. King B, Trimarchi T, Reavie L, et al. The ubiquitin ligase FBXW7 modulates leukemia-initiating cell activity by regulating MYC stability. *Cell.* 2013;153(7):1552-1566.

53. Takada M, Zhang W, Suzuki A, et al. FBW7 loss promotes chromosomal instability and tumorigenesis via cyclin E1/CDK2-mediated phosphorylation of CENP-A. *Cancer Res.* 2017;77(18):4881-4893.

54. De Keersmaecker K, Atak ZK, Li N, et al. Exome sequencing identifies mutation in CNOT3 and ribosomal genes RPL5 and RPL10 in T-cell acute lymphoblastic leukemia. *Nat Genet.* 2013;45(2):186-190.

55. Song JH, Schnittke N, Zaat A, Walsh CS, Miller CW. FBXW7 mutation in adult T-cell and B-cell acute lymphocytic leukemias. *Leuk Res.* 2008;32(11):1751-1755.

56. Malyukova A, Dohda T, von der Lehr N, et al. The tumor suppressor gene hCDC4 is frequently mutated in human T-cell acute lymphoblastic leukemia with functional consequences for Notch signaling [published correction appears in *Cancer Res.* 2008;68(6): 2051]. *Cancer Res.* 2007;67(12):5611-5616.

57. O'Neil J, Grim J, Strack P, et al. FBW7 mutations in leukemic cells mediate NOTCH pathway activation and resistance to gamma-secretase inhibitors. *J Exp Med.* 2007;204(8): 1813-1824.

58. Galli F, Rossi M, D'Alessandra Y, et al. MDM2 and Fbw7 cooperate to induce p63 protein degradation following DNA damage and cell differentiation. *J Cell Sci.* 2010;123(pt 14): 2423-2433.

59. Caserta TM, Kommagani R, Yuan Z, Robbins DJ, Mercer CA, Kadakia MP. p63 overexpression induces the expression of Sonic Hedgehog. *Mol Cancer Res.* 2006;4(10): 759-768.

60. Kadri S, Lee J, Fitzpatrick C, et al. Clonal evolution underlying leukemia progression and Richter transformation in patients with ibrutinib-relapsed CLL. *Blood Adv.* 2017; 1(12):715-727.

61. Landau DA, Sun C, Rosebrock D, et al. The evolutionary landscape of chronic lymphocytic leukemia treated with ibrutinib targeted therapy. *Nat Commun.* 2017;8(1):2185.

62. Hatzi K, Jiang Y, Huang C, et al. A hybrid mechanism of action for BCL6 in B cells defined by formation of functionally distinct complexes at enhancers and promoters. *Cell Reports.* 2013;4(3):578-588.

63. Tiberi L, Bonnefont J, van den Ameele J, et al. A BCL6/BCOR/SIRT1 complex triggers neurogenesis and suppresses medulloblastoma by repressing Sonic Hedgehog signaling [published correction appears in *Cancer Cell.* 2015;27(2):312-313]. *Cancer Cell.* 2014;26(6): 797-812.

64. Ghetu AF, Corcoran CM, Cerchietti L, Bardwell VJ, Melnick A, Privé GG. Structure of a BCOR corepressor peptide in complex with the BCL6 BTB domain dimer. *Mol Cell.* 2008;29(3):384-391.

65. Coni S, Antonucci L, D'Amico D, et al. Gli2 acetylation at lysine 757 regulates hedgehog-dependent transcriptional output by preventing its promoter occupancy. *PLoS One.* 2013;8(6):e65718.

66. Zhou H, Kim S, Ishii S, Boyer TG. Mediator modulates Gli3-dependent Sonic hedgehog signaling. *Mol Cell Biol.* 2006;26(23): 8667-8682.

67. Kämpjärvi K, Järvinen TM, Heikkinen T, et al. Somatic MED12 mutations are associated with poor prognosis markers in chronic lymphocytic leukemia. *Oncotarget.* 2015;6(3):1884-1888.

68. Turunen M, Spaeth JM, Keskitalo S, et al. Uterine leiomyoma-linked MED12 mutations disrupt mediator-associated CDK activity. *Cell Reports.* 2014;7(3):654-660.

69. Kämpjärvi K, Park MJ, Mehine M, et al. Mutations in exon 1 highlight the role of MED12 in uterine leiomyomas. *Hum Mutat.* 2014;35(9):1136-1141.

70. Dagklis A, Demeyer S, De Bie J, et al. Hedgehog pathway activation in T-cell acute lymphoblastic leukemia predicts response to SMO and GLI1 inhibitors. *Blood.* 2016; 128(23):2642-2654.

71. Singh RR, Kim JE, Davuluri Y, et al. Hedgehog signaling pathway is activated in diffuse large B-cell lymphoma and contributes to tumor cell survival and proliferation. *Leukemia.* 2010; 24(5):1025-1036.

72. Singh RR, Cho-Vega JH, Davuluri Y, et al. Sonic hedgehog signaling pathway is activated in ALK-positive anaplastic large cell lymphoma. *Cancer Res.* 2009;69(6):2550-2558.

73. Hegde GV, Munger CM, Emanuel K, et al. Targeting of sonic hedgehog-GLI signaling: a potential strategy to improve therapy for mantle cell lymphoma. *Mol Cancer Ther.* 2008;7(6):1450-1460.

74. Dierks C, Grbic J, Zirlik K, et al. Essential role of stromally induced hedgehog signaling in B-cell malignancies. *Nat Med.* 2007;13(8): 944-951.